Hydraulic and Strength Properties of Unexposed and Freeze/Thaw Exposed Cement-Stabilized Soils

Reza Jolous Jamshidi[1] and Craig B. Lake[2]*.

[1]Ph.D. Candidate, Civil and Resource Engineering Department, Dalhousie University, Canada.

E-mail: jolous@dal.ca.

[2]Associate Professor and Head, Civil and Resource Engineering Department, Dalhousie University, Canada.

*Corresponding author. E-mail: craig.lake@dal.ca, Tel.: +1 (902) 494 3220.

Abstract

A total of 108 specimens were prepared to examine the hydraulic and strength performance of nine different cement-stabilized soils under unexposed and freeze/thaw (f/t) exposed conditions. Specimens from each mix design were evaluated under two levels of curing conditions (i.e. immature vs. mature). Hydraulic conductivity and unconfined compressive strength (UCS) measurements were performed to assess changes in the performance of specimens after 12 cycles of freezing at -10±1^{o}C and thawing at 22±1^{o}C. Measured mass losses of the specimens from a standard brushing test was also monitored at different f/t cycles and results were compared to the changes in the hydraulic performance for each mix design. Hydraulic conductivity measurements on unexposed mature specimens showed that the lowest values likely occur at water contents slightly wet of optimum water content (OWC). UCS values showed a general decreasing trend with the increase in the water content for both immature and mature specimens under unexposed conditions. After f/t exposure specimens showed minor reductions as well as increases of up to 5250 times in hydraulic conductivity values. Increases of up to 14 percent and reductions of up to 58 percent in compressive strength were also observed compared to unexposed conditions. For most cases, mature specimens resulted in a higher degree of damage compared to immature specimens. Results from the brushing tests showed this test method is not a suitable indicator for predicting changes in the hydraulic performance of cement-stabilized soils. Hydraulic conductivity measurements after a period of post-exposure healing showed damaged specimens have some potential in recovering parts of the increased hydraulic conductivity value due to the healing process.

Keywords: Freeze, Thaw, Soil-Cement, Stabilization, Hydraulic conductivity, Compressive strength.

1. INTRODUCTION

Cement-based stabilization is widely used for improving the engineering properties of problematic soils. Although the majority of these soil improvement projects focus on increasing the strength related properties of the initial materials (e.g. soil-cement used as a base material for pavements, foundation stabilization, slope protection, etc.) (ACI 1990), there are many applications in which the hydraulic conductivity of the final product is a concern. Canal linings, vertical cut-off walls, and cement-based solidification/stabilization remediation projects are a few examples of such applications.

Hydraulic conductivity measurement of cement-stabilized soils has been the subject of studies by Ganjian et al. (2004), Bellezza & Fratalocchi (2006), and Hammad (2013). However, there has been few studies evaluating the influence of environmental exposures such as cycles of freeze/thaw (f/t) on the hydraulic performance of cement-treated materials. Based on evaluation of limited number of specimens, Pamukcu et al. (1994) showed minor reductions as well as increases of up to two orders of magnitude in the hydraulic conductivity of cement-stabilized dewatered sludge after 12 f/t cycles. To predict hydraulic conductivity of compacted soil-cement after one f/t exposure, Shea (2011) proposed an equation based on basic soil characteristics, cement content, and the 7 day UCS value.

In absence of sufficient literature and reliable standards, many cement-stabilization projects (i.e. durability studies and project performance specifications) where changes in hydraulic conductivity may be critical to performance, suggest percent mass loss as an indicator for evaluating acceptance of performance under f/t exposure (e.g. Paria & Yuet 2006; ITRC 2011).

There are two drawbacks to this approach. Firstly, mass loss does not necessarily correspond to internal changes in the structure of cemented soils, which in essence controls the hydraulic conductivity of these materials (El-Korchi et al. 1989). Secondly, the actual performance degradation of the stabilized soil is not quantified, as the results do not provide any quantitative information on the changes in hydraulic conductivity of the material being tested. In other words, mass loss may be able to establish that there is damage to the specimen after f/t, but the extent of the damage will be unknown.

Jolous Jamshidi (2014) studied the effect of f/t testing conditions such as freezing temperature (-2, -10, and -20^{o}C), curing age at the time of first f/t cycle (16 and 35 days), and number of f/t cycles (4 and 12 cycles) on hydraulic and strength performance of a cement-stabilized silty sand. Increases of up to three orders of magnitude in hydraulic conductivity as well as strength loss of up to 95 percent in the unconfined compressive strength (UCS) values were reported in the study. Statistical analyses performed on the results showed that all of the investigated testing factors were significant in the observed changes in the hydraulic conductivity and UCS values. It was also suggested that modifications in the mix design (i.e. increasing the cement content or reducing the water content) may result in better performance of cement-stabilized soils under f/t exposure.

The current paper investigates the influence of a soil's grain size distribution (i.e. fines content), soil-cement water to cement (w/c) ratio, and curing age on the hydraulic and strength properties of cement-stabilized soils under control (i.e. unexposed) and f/t exposed conditions. Given the lack of literature on hydraulic performance of soil-cement, measurements on control conditions were necessary to better evaluate the influence of mix design on the f/t exposed specimens. The efficiency of the mass loss measurement in predicting changes in hydraulic performance of damaged specimens is also discussed. The potential healing capacity of f/t damaged specimens in recovery of their increased hydraulic conductive is also examined for some of the specimens that underwent damage during f/t.

2. MATERIALS AND METHODS

2.1 Soil materials

The three soils examined in this work were lab-manufactured by blending together “soil A” and “soil B” at different proportions, as presented in Table 1. Soil A consisted of a glacially derived silty sand (ASTM-D2487 2011) from Halifax, Nova Scotia that was initially sieved through a 9.5 mm (ASTM-D6913 2004) mesh-sized sieve to remove oversized material. The remaining soil was then passed through 4.75, 1.20, 0.30, and 0.08 mm sieves. The portion remaining on the 0.08 mm sieve was washed through this sieve (with wash water being discarded) in order to minimize the amount of fines content in this soil. Soil B was prepared by sieving a silt material derived from quarry operations through a 0.08 mm sieve and discarding the oversized portion. The graded materials from both soils were stored in plastic bags for future blending according to each mix design. The separation of the soils into specific gradation ranges provided some control on grain size distribution between different soil-cement mix designs.

Results of mineral oxides analyses for soil A and soil B are presented in Table 2. For both soils, silica and aluminum are the major oxides present, which account for more than 80% of the total composition. Ignition of the soil A and soil B at 1000^{o}C yielded a loss on ignition (LOI) of 2.41 and 1.17%, respectively, indicating the presence of small amounts of organic matter in these soils. X-ray diffraction tests performed on soil A and B samples (<0.044 mm size fraction) showed quartz and feldspars as the main mineralogical components of these materials.

Standard proctor compaction tests (ASTM-D558 2011) were performed on each soil (i.e. Soil I, II, and III) blended with 10% cement to identify the optimum water content (OWC) of the resulting soil-cement. As presented in Figure 1, the three soils show an OWC in the range of 8 to 11% and a maximum dry density ranging from 1976 to 2050 Kg/m^3. Slight increases in the OWC and slight decreases in the maximum dry density were observed with an increase in the fines content (passing 0.08 mm sieve) in the soils.

2.2 Soil-cement specimen preparation

A total of nine mix designs were used in this research (see Table 1). Specimens were prepared by addition of 10% (i.e. cement/dry mass of soil) general use Portland-limestone blended cement (CSA type GUL) to each soil at different w/c ratios (i.e. 1, 1.5, and 2). Examination of the water content of the soil-cement mixture relative to the OWC, as well as some visual pre-assessment of the workability of the mixes, were performed to determine if specimens would be either compacted in standard compaction molds (ASTM-D558 2011) or placed into plastic molds for self-consolidation (Table 1). A brief description for each of these specimen preparation methods is provided in the following sections.

2.2.1 Compaction method for dry soil-cement specimens

The required soil for each set of mix design was prepared by mixing soil A and B according to proportions presented in Table 1. Cement was then added to the soil and mixed until the mixture became homogeneous. The amount of water required to reach the target total w/c ratio, calculated by incorporating the moisture content of the soil before mixing, was then added to the soil-cement blend. Mixing was performed using a drill-mounted paddle until a uniform mixture was reached. The resulting soil-cement was compacted in standard proctor molds in three layers with each layer subjected to 25 blows of a 2.49 Kg standard hammer following ASTM-D558 (2011). After compaction, the molds were placed in sealed plastic bags (to minimize water evaporation) for 5 days prior to extrusion. Specimens were then stored in a 100% humidity moist room until the required age of testing.

2.2.2 Self-consolidation method for wet soil-cement specimens

For the wet mixing preparation of specimens, dry cement and water were first proportioned at the required w/c ratio and then mixed to form a slurry. The soil was then incrementally added to the cement slurry and mixed uniformly via a drill-mounted paddle. The given soil-cement mixture was then placed into cylindrical plastic molds with a nominal size of 101 mm diameter and 118 mm height. The soil-cement placement occurred in three layers, each layer being subjected to 20 strokes using a standard concrete slump testing rod to provide consistent consolidation. Similar to the dry mix preparation method, molds were placed in a sealed plastic bag for 5 days prior to extrusion. Specimens were then kept in a 100% humidity moist room prior to further testing.

2.3 F/t conditioning of soil-cement specimens

Specimens from each mix design were exposed to f/t cycles at immature and mature curing conditions. The first f/t cycle exposure occurred at the age of 16 days for immature and over 110 days for mature curing conditions. F/t cycling consisted of approximately 24 hours of freezing in a freezer set at -10±1°C followed by thawing in a 100% humidity room at a temperature of 22±1°C. All specimens were saturated under a minimum backpressure of 524 KPa (with a confining pressure of 558 to 593 KPa) for a minimum of seven days prior to f/t exposure (ASTM-D5084 2010).

2.4 Specimen testing

The testing program was designed to evaluate the physical performance of both unexposed and exposed specimens for different mix designs and curing maturities. Figure 2 presents the sequence of testing for both immature and mature curing conditions. Tests performed on the 12 specimens from each mix design are also presented in Table 3. Details of the testing conditions used in the study are also discussed in the following sections.

2.4.1 Hydraulic conductivity

Hydraulic conductivity measurements were performed on duplicate specimens following method A of ASTM-D5084 (2010) (i.e. constant head flexible-wall method). Permeation with de-aired water was performed under a hydraulic gradient ranging from 11 to 116 depending on the permeability of the specimens in order to control the length of experiments. Test durations ranged from 3 days for highly damaged specimens after f/t exposure, to 2 weeks for low permeable mature specimens. An outflow to inflow ratio of between 0.75 to 1.25 and a steady hydraulic conductivity value were considered as the test termination criteria. For specimens with very low hydraulic conductivity (i.e. less than 5×10^{-11} m/s), the outflow to inflow ratio was difficult to achieve in the two-week period of the testing, hence these tests were terminated when a steady hydraulic conductivity value was reached in consecutive readings.

For immature tests, control hydraulic conductivity values (K_0) were measured on specimens (specimens 1 and 2 in Figure 2 (a)) after approximately 9 days from specimen preparation. This test was completed before day 16, when the f/t cycling of these specimens began. At the end of the 12th f/t cycle, these same specimens were tested for hydraulic conductivity values for exposed conditions ($K_{exposed}$). The hydraulic conductivity ratio, defined as the ratio of hydraulic conductivity values of exposed specimens to the values obtained prior to f/t exposure ($K_{exposed}/K_0$), are used subsequently to discuss changes in the hydraulic performance of specimens after f/t exposure.

For mature tests, control hydraulic conductivity values (K_0) were measured after about 95 days from specimen preparation (specimens 7 and 8 in Figure 2 (b)). At the completion of the test, specimens were exposed to 12 f/t cycles. Similar to immature specimens, hydraulic conductivity measurements were performed on exposed specimens and the hydraulic conductivity ratio was calculated to assess the changes in the performance of specimens after exposure to f/t cycles.

2.4.2 Percent mass loss

Current industry practice suggests percent mass loss as an indicator of resistance of cement-stabilized soils exposed to f/t cycles. To evaluate the reliability of this method in terms of predicting the changes in hydraulic performance of soil-cement, the brushing test (as suggested by ASTM-D560 (2003)) was performed on duplicate specimens (specimens 3 and 4 in Figure 2 (a), 9 and 10 in Figure 2 (b)) at the end of each f/t cycle and the specimens' mass was recorded. Brushing consisted of 20 strokes on the sides of the specimens (covering the perimeter twice) and 4 strokes on the top and bottom side of the specimens using a wire brush. Changes in the mass of the specimens were monitored by calculating the percent mass loss (Δ_m) using the following equation:

$$\Delta_m = \frac{m_i - m_m}{m_i} \times 100 \qquad \text{Equation 1}$$

where m_i and m_m are the initial mass and mass of the specimen after brushing at the end of the m^{th} cycle, respectively.

2.4.3 Unconfined compressive strength (UCS)

Unconfined compressive strength (UCS) measurements were performed on duplicate specimens under unexposed (i.e. control) (specimens 5 and 6 in Figure 2 (a), 11 and 12 in Figure 2 (b)) and exposed conditions (specimens 3 and 4 in Figure 2 (a), 9 and 10 in Figure 2 (b)). For exposed conditions, the same specimens used for brushing tests were tested for UCS and as a result the reported values represent the residual compressive strength of the specimens after the brushing test. The UCS ratio is calculated by dividing the average UCS values for exposed specimens by the average of values for unexposed specimens. In order to minimize variability between tests, UCS measurements for both exposed and unexposed specimens were performed on the same day. All specimens were sulfur-capped prior to the test to ensure concentric loading during the test. UCS values were obtained using a vertical deformation rate of 0.5 mm/min.

It is known that the hydration of cement occurs at a very slow rate at sub-zero temperatures (Kosmatka et al. 2003). Comparing the testing procedures for measuring UCS values of control (unexposed) and exposed specimens in Figure 2 (a) and (b) shows that exposed specimens cure for about 12 days less than unexposed specimens due to the 12 f/t cycles (assuming minimal curing during each freezing period). For mature specimens, considering the length of the experiments (over 134 days), the curing age difference between control and exposed specimens will have a negligible effect on the observations. However, for immature specimens, to minimize the possible influence of this difference on UCS values, tests were performed approximately 20 days after completion of f/t cycles (curing compensation period in Figure 2 (a)). This ensured at least 48 days of curing for both control and exposed specimens in immature UCS tests. At this age it is assumed that differences observed in the results are due to the f/t cycling of exposed specimens as opposed to lack of curing in these specimens.

Considering the length of time required for f/t cycling and the curing compensation period (only for immature specimens), UCS tests for control conditions were performed at about 60 days after specimen preparation for immature tests and after 134 days for mature tests. To provide additional information on the effect of shorter and longer curing times on UCS than that described above, another specimen set was prepared for mixes SI(1), SI(2), SIII(1), and SIII(2) (selected as extreme mix designs for fine content and w/c ratio) and was tested for UCS values at the age of 16 days and 241 days.

2.5 Hydraulic conductivity recovery of exposed specimens

In contrast to exposure to f/t cycles, which is believed to damage the structural integrity of porous materials, autogenous healing has been reported to act positively in durability of cement–based materials (e.g. Jacobsen & Sellevold 1996) and soils (e.g. Eigenbrod 2003). To study the possibility for autogenous healing with respect to hydraulic conductivity changes after f/t exposure, 10 immature and mature specimens (i.e. immature specimens from SI(1.5), SII(1.5), and SII(2) mix designs and mature specimens from SI(1.5) and SI(2) mix designs) which exhibited highest amounts of hydraulic conductivity changes during the experiments were re-tested for hydraulic conductivity values after a post-exposure curing period of at least 120 days in the moist room. Hydraulic conductivity ratios for healed specimens (i.e. K_{healed}/K_0) are calculated and compared to hydraulic conductivity ratios for the same specimens measured at the end of the 12^{th} f/t cycle (i.e. $K_{exposed}/K_0$).

3. RESULTS AND DISCUSSION

Results of the testing described above are presented in following three sections. Firstly, the effect of mix design and level of curing on hydraulic and strength performance of cement-stabilized soils is presented (i.e. comparing the changes in the performance between unexposed specimens). Secondly, changes in hydraulic and strength performance of specimens after exposure to f/t cycles are presented and compared to values obtained from control conditions. This section also compares the changes in hydraulic conductivity values due to f/t exposure to the brushing tests results. Thirdly, the healing potential of exposed specimens are evaluated by presenting the changes in hydraulic conductivity values of damaged specimens after post-exposure curing.

3.1 Comparison of performance among control specimens

3.1.1 Influence of w/c ratio on hydraulic conductivity and UCS

There is limited data in the literature related to the hydraulic conductivity of cement-stabilized soils and its relation to changes in the w/c ratio. Hammad (2013) performed laboratory studies on the effect of molding water content on hydraulic conductivity of a cement-stabilized silty sand. Hammad (2013) found that the lowest hydraulic conductivity for specimens cured for 28 days occurs at a water content ranging from 2 to 6 percent above the OWC measured from the standard proctor test. Extensive studies on compacted clays also exist in the literature that show the minimum hydraulic conductivity occurs at a water content slightly wet of OWC from standard proctor compaction effort (e.g. Boynton & Daniel 1985; Haug & Wong 1992).

Based on the standard compaction test results for this study presented in Figure 1, specimens prepared at the w/c ratio of 1.5 (i.e. SI(1.5), SII(1.5), and SIII(1.5)) fall within the water content range of 2 to 6 percent wet of OWC (i.e. hatched areas in Figure 1). Figure 1 shows that, with the exception of the immature specimens for SI(1.5) and SII(1.5), these specimens have the lowest hydraulic conductivity values in comparison to other mix designs for both immature and mature conditions. Immature specimens for SI(1.5) and SII(1.5) both have hydraulic conductivity values higher than specimens with lower w/c ratio. This different behavior is likely due to high amounts of available water in the mix design of these specimens (due to the lower fines content of the initial soils) that delays the time required to disconnect the pore structure (Powers et al. 1959; Hearn et al. 2011). Even for these specimens, at longer curing times (i.e. mature specimens), the lowest measured hydraulic conductivity occurs at w/c ratio of 1.5 (i.e. 2 to 6 percent wet of optimum water content).

Specimens from the SIII(1) mix design, which were compacted dry of optimum water content, exhibit hydraulic conductivity values of over two orders of magnitude higher than those compacted at slightly wet of optimum. This shows deviation from OWC towards a drier mix design can drastically increase the expected hydraulic conductivity values for both immature and mature conditions. Similar observations have been reported in previous studies on compacted clays (e.g. Mitchell et al. 1965; Boynton & Daniel 1985). This is likely a result of insufficient lubrication of soil and cement particles during the compaction process at these low water contents which results in poor kneading compaction.

The w/c ratio and its importance as an indicator for mix design strength has been widely studied for concrete (Popovics & Ujhelyi 2008). According to Abram's theory (Abrams 1919), provided that a minimum w/c ratio required for the hydration of available cement and the workability of concrete is available in a mix design, further increase in w/c ratio results in reduction of the compressive strength.

Results of UCS tests on cement-stabilized clays by Aderibigbe et al. (1985) showed a bell shape relation between w/c ratio and UCS. Optimum w/c ratios, to achieve the highest UCS, ranged from 0.4 to 2.6 for different ratios of cement/clay. Horpibulsuk et al. (2010) conducted some experiments to study the relation between the OWC for UCS and density (i.e. standard proctor test). Results showed that while for an un-cemented clay, the OWC for UCS and density were similar, for cemented samples the maximum strength occurred at about 1.2OWC from proctor test results. Horpibulsuk et al. (2003) also showed that Abram's equation is valid to predict the compressive strength of cemented clay with respect to w/c ratio at high water contents. Experiments by Guney et al. (2006) on cemented non-plastic soils (i.e. foundry sand) for w/c ratios ranging from 2% dry of to 2% wet of proctor test OWC, showed a general decreasing trend for UCS. This possibly suggests similarities between non-plastic soils and concrete in terms of w/c ratio-UCS behavior with respect to OWC from compaction tests (i.e. requiring minimum hydration water and workability as opposed to following the trends of proctor test OWC results).

For the three soils investigated in this study, all the w/c ratios, with the exception of SIII(1) specimens, are on the wet side of the material's OWC. UCS results (Figure 1) for the three soils show a general decreasing trend in compressive strength values as a result of an increase in the water content.

3.1.2 Effect of curing age (immature vs. mature)

Cement-based materials have a dynamic structure that changes with time due to the ongoing process of cement hydration. According to Powers & Helmuth (1953) the pore size distribution within the structure of a cement paste can be divided into gel pores, capillary pores, and air voids. Water permeation in cement-based materials mainly occurs through a network of capillary pores, and air voids. At the early stages of hydration, capillary pores are connected and provide a permeable medium. As the hydration process continues, some of the capillary pores change into gel pores and become disconnected, resulting in significant reduction in hydraulic conductivity. Powers et al. (1954) showed a reduction of over six orders of magnitude can occur in the hydraulic conductivity of cement paste from the time of specimen preparation (i.e. fresh paste) until 24 days of curing. The hydration process also causes an increase in the strength of the cemented soils because of the increased binding capacity of cement paste (ACI 1990).

Comparing the hydraulic conductivity results for immature (16 days of curing) and mature (over 95 days of curing) conditions, Figure 1 shows a decrease of up to two orders of magnitude in the values at the longer curing age. However, UCS results in Figure 1 show a negligible difference between the values obtained for immature and mature control tests (with some cases immature specimens showing slightly higher UCS values compared to mature specimens). The reason for the minor difference between these cases is that, unlike the hydraulic conductivity specimens, UCS measurements for these control specimens were performed at an age of about 60 days for immature specimens (after completion of f/t cycling and curing compensation period (see Figure 2)), at which the main portion of hydration process is likely completed.

To provide some insight on the UCS values for shorter and longer curing ages, a parallel set of tests including mix designs from extreme conditions (lowest and highest w/c ratios and fines contents: i.e. SI(1), SI(2), SIII(1), and SIII(2)) was conducted. UCS measurements were performed on specimens at the age of 16 and 241 days. Results are presented in Figure 3, and show an increase of up to 52 percent in the UCS values between extreme curing ages (16 and 241 days). Considering the results of control specimens (from immature and mature tests) presented in Figure 3, a general increasing trend can be observed for most of the mix designs. The exceptions are specimens from SIII(1), which show no obvious trend in the values. Considering that these specimens were cast at dry of OWC, this could be due to the low workability of this mix design resulting in a higher heterogeneity in the observed values.

3.2 Influence of f/t exposure on the performance (i.e. exposed conditions)

Performance of specimens after exposure to f/t cycles are presented in the current section. In discussing the behavior of exposed specimens herein, immature and mature exposed specimens are referred as immature and mature specimens, respectively.

3.2.1 Hydraulic conductivity

Figure 4 shows the results of hydraulic conductivity measurements for specimens after exposure to f/t cycles. In terms of hydraulic conductivity changes, Figure 4 shows both minor reductions for some immature specimens (i.e. hydraulic conductivity ratios less than 1) and increases of up to 5250 times. The increase in the hydraulic conductivity values can be attributed to the formation of cracks/micro-cracks within the structure of cement-stabilized soil during the freezing process. Any reduction in the hydraulic conductivity values after f/t is likely a result of the continuing hydration process in immature specimens that offsets any deteriorating effect of f/t cycles.

For soil I, specimens compacted near the OWC show the least amount of changes for both immature and mature conditions. It is expected that increase in water content in the mix design will result in higher f/t susceptibility of specimens (due to the reduced strength and increased porosity of the specimens) and hence increase in hydraulic conductivity ratios. According to Figure 4 (a), this trend is true with the exception of immature specimens at w/c ratio of 2. For these specimens, a reduction in hydraulic conductivity ratio was observed in comparison with the specimens prepared at w/c ratio of 1.5. This behavior could be due to interference of the hydration process with deteriorating effect of freezing exposure in these specimens. Another possible reason for this behavior can be the high initial hydraulic conductivity of specimens from this mix design that can facilitate water transport through the soil-cement structure. This can prevent development of hydraulic pressure in the specimens during the freezing process and reduce the amount of observed damages (Powers & Willis 1949).

For soil II (Figure 4 (b)), an increase in the hydraulic conductivity ratio is evident as a result of increased w/c ratio in immature specimens. For mature specimens, while hydraulic conductivity ratio is noticeably higher for specimens prepared at w/c ratio of 2, specimens with w/c ratio of 1 and 1.5 exhibit relatively similar changes in hydraulic conductivity values.

For soil III (Figure 4 (c)), even though there are increasing trends in the hydraulic conductivity ratios for mature specimens with the increased w/c ratio, values of hydraulic conductivity for immature specimens after f/t exposure are very similar to values measured for control conditions (i.e. hydraulic conductivity ratios close to 1). Comparing the hydraulic conductivity ratio for immature and mature specimens in Soil III to similar w/c ratios for Soil I and Soil II also shows better or relatively similar performance for this soil due to higher fines content.

From the results in Figure 4, it is also evident that mature specimens undergo a higher degree of damage (in terms of changes in hydraulic conductivity values) as compared to immature specimens. This is in agreement with observations by the authors in a previous publication (Jamshidi 2014). Higher damage in mature specimens is likely a result of their increased brittleness due to the hydration process, which makes the material more sensitive to the deformations caused during the freezing exposure. The progressive hydration process in immature specimens may also offset the deteriorating effect of freezing, which can result in less changes in the observed hydraulic conductivity values.

Othman et al. (1994) showed that for compacted clays, specimens with higher initial hydraulic conductivity exhibit lower increases in hydraulic conductivity values after f/t exposure. For the specimens tested in this study, variation of hydraulic conductivity ratios after f/t exposure are plotted against initial hydraulic conductivity in Figure 5. While there is no obvious trend in the results, it seems that (although there are limited data points available) for initial hydraulic conductivity values higher than 1×10^{-8} m/s, relatively small changes in the hydraulic conductivity may occur after f/t exposure.

3.2.2 Brushing test

The results of the brushing tests performed on exposed specimens at different f/t cycles is presented in Table 4. A mass loss (Δ_m) of between 0.72 to 23.4 percent was observed at the end of the 12th f/t cycle. However, it should be noted that all the experiments, with the exception of SII(2)-mature, showed a mass loss of less than 7 percent. This is despite hydraulic conductivity increases of up to three orders of magnitude for some of these mix designs. By comparing the mass loss data to the hydraulic conductivity changes presented in previous section, we can also conclude that the amount of mass loss in specimens is not proportional to the changes in the hydraulic conductivity values. For instance, specimens from SII(2)-immature and SII(1)-immature exhibit approximately equal mass loss at the end of the 12th f/t cycle, however, hydraulic conductivity ratios for these mix designs show about 100 times increase for SII(2)-immature and 15% reduction for SII(1)-immature. This difference is mainly because mass loss data represent the changes in the surface of the exposed specimens, while hydraulic conductivity is controlled by internal changes in the specimens.

Comparing the results of mass loss at the end of the 12th f/t cycle for immature and mature curing conditions (Figure 6), shows a higher degree of surface damage in mature specimens after the brushing test. This is consistent with the observations for hydraulic conductivity changes (i.e.

higher increases for mature specimens) presented in the previous section. Figure 6 also shows an increase in w/c ratio seems to result in higher amount of mass loss for both immature and mature specimens. The exception to this observation being SII(1) and SII(1.5) specimens, which both have very low mass loss values of less than 3 percent. The increase in the mass loss due to the increased w/c ratio may partially be a result of decreased UCS values (and consequently tensile strength) of these specimens, which makes them more vulnerable to surface damages due to the brushing test.

3.2.3 Unconfined compressive strength

Figure 7 presents the results of UCS tests on specimens after exposure to f/t cycles. Reductions as high as 58 percent as well as increases as high as 14 percent were observed after f/t exposure. There is no clear trend in the changes in the observed values with regards to the mix design and water content. However, for most cases of immature and mature exposure (with the exception of SIII(1)-immature), compressive strength values still follow the same trend as control conditions (i.e. decreasing value with the increase in water content). SIII(1)-immature specimens showed 58 percent reduction in the compressive strength, resulting in UCS values smaller than SIII(1.5) and SIII(2) mix designs. This difference in the behavior suggests specimens compacted at dry of OWC may be more sensitive (in terms of UCS changes) to the exposure of freezing conditions at younger curing ages.

Considering the UCS ratios presented in Figure 7 (a) for soil I, specimens prepared at the w/c ratio close to the OWC resulted in minor changes after f/t exposure (UCS ratios close to 1). Also, an increase in w/c ratio in the mix designs for this soil seems to result in higher amounts of damage (i.e. lower UCS ratios) for both immature and mature cases with the exception of SI(2)-immature. This is in agreement with the changes in the hydraulic conductivity values for this mix design, which were presented in section 3.2.1.

For soil II (Figure 7 (b)), UCS ratios decrease (i.e. higher damage) as a result of increase in w/c ratio, with the exception of SII(1)-immature. For the SII(1) mix design, while mature specimens exhibited a UCS ratio of 1.14 (showing increase in the strength), immature specimens showed a decrease of approximately 30 percent (i.e. UCS ratio of 0.71) in the UCS values after f/t exposure. The poor performance of immature specimens for this mix design (compared to higher w/c ratios) is likely due to incomplete structure of these specimens at the time of exposure as a result of low w/c ratio. This is in agreement with the reductions observed in the hydraulic conductivity of SII(1)-immature after f/t exposure, which indicates continuation of curing process for these specimens.

For soil III (Figure 7 (c)), mature specimens compacted dry of OWC show an increase in UCS values after f/t exposure, while immature specimens from the same mix design exhibit about 58 percent reduction in UCS values compared to control conditions. Specimens prepared at higher w/c ratios exhibit UCS values similar to control conditions (i.e. UCS ratios close to 1), with the exception of mature specimens from SIII(1.5) that show about 20 percent reduction in UCS values after f/t exposure.

Dempsey & Thompson (1973) previously showed that there is a good correlation between UCS values for f/t exposed specimens (after 5 and 10 f/t cycles) and results of vacuum saturated UCS tests on unexposed specimens. The relation between exposed and unexposed UCS values in the current study is presented in Figure 8. A coefficient of determination (R^2) of 80 percent between the results suggests that unexposed UCS can be used to predict strength changes in the soil-cement after f/t exposure.

Comparing the changes in the UCS and hydraulic conductivity values after exposure to f/t cycles doesn’t show any correlation between the observed data. For instance, while SII(1)-mature specimens show an increase of about 50 times in hydraulic conductivity values after f/t exposure, specimens from the same mix design show a strength gain of about 14 percent. Similarly, while hydraulic conductivity of SII(1)-immature decreased after f/t exposure (i.e. improved performance), a reduction of 30% is observed in UCS test results (i.e. performance degradation). These variations could be due to the different nature of these tests. For a specific mix design, f/t conditioning of the specimens may result in an increase in the porosity of the structure that can lead to a reduction in the compressive strength values. However, increase in the hydraulic conductivity, depends on the amount of connected porosity (including cracks and micro cracks) in the structure. Contrary, even a local crack can result in considerable increase in the hydraulic conductivity values, but possibly a smaller change in the observed UCS values.

3.3 Healing potential for exposed specimens

Many mechanisms have been suggested to result in the self-healing healing of cement-based materials after f/t exposure. Those include further hydration of un-reacted cement, crystallization (calcium carbonate), or clogging of the cracks due to the impurities in the flow or moving of loose particles in the matrix (Edvardsen 1999). A study by Jacobsen & Sellevold (1996) showed a partial regain of compressive strength of frost damaged concrete after a period of submersion in water. Microstructural observations by Jacobsen et al. (1995) showed the presence of newly formed C-S-H, ettringite, and calcium hydroxide in the cracks after the healing period. A study by Yang et al. (2009) on concrete suggests that the recovery of mechanical and transport properties of the samples can only be achieved under conditions of extremely tight crack widths. Under these conditions, full recovery for crack widths of less than 50 μm and partial recovery for crack width of up to 150 μm was achieved.

To study the potential for hydraulic conductivity recovery of specimens after f/t exposure, ten specimens (from both immature and mature curing conditions) that exhibited hydraulic conductivity ratios ($K_{exposed}/k_0$) ranging from 5.4 to 5250 were re-tested for hydraulic conductivity, after a post-exposure curing period of over 120 days in the moist room (K_{healed}). The healed hydraulic conductivity ratio was calculated by dividing values after the post exposure curing period by the control conditions (K_{healed}/K_0). Comparing the results to the values for control and exposed specimens (Figure 9) shows a wide range of healing potential for hydraulic conductivity values. Multiplier numbers next to the arrows on Figure 9 show the hydraulic conductivity ratios for exposed and healed specimens.

For immature conditions, SI(1.5) specimens which had hydraulic conductivity ratios of less than 50 times (49.2 and 43.5 for specimens #1 and # 2, respectively) after f/t cycles, recovered to hydraulic conductivity ratios of 5.5 and 2.0 after the healing period. SII(1.5)-immature specimens also healed from hydraulic conductivity ratios of 7.8 and 5.4 after f/t, to hydraulic conductivity ratios of 1.7 and 2.3, respectively. On the other hand, SII(2)-immature specimens which exhibited hydraulic conductivity ratios of 75 and 112.5 after f/t exposure, reached to hydraulic conductivity ratios of 13.5 and 54.2 after the healing period, respectively.

Mature specimens from SI(1.5) and SI(2) mix designs showed hydraulic conductivity ratios of about 300 to 5200 after f/t exposure. After the post exposure healing period, even though these specimens exhibited some reduction in the hydraulic conductivity values compared to exposed conditions, results are still over two orders of magnitude higher than similar measurements for control conditions (Figure 9).

Results of immature and mature specimens from Figure 9 could indicate that highly damaged specimens have less potential in recovery of lost hydraulic conductivity values, potentially due to formation of larger crack widths in their structure similar to observations by Yang et al. (2009).

4. SUMMARY AND CONCLUSIONS

The current study investigated the influence of fines content in a soil, w/c ratio in soil-cement mix design, and curing conditions on performance of cement-stabilized soils prior to, and after, exposure to 12 cycles of f/t. A summary of the findings is as follows:

1. Hydraulic conductivity measurements for unexposed specimens showed that minimum values can likely be achieved at a w/c ratio slightly wet of OWC, as was previously suggested in the literature (Hammad 2013). Also, comparing the results of immature and mature hydraulic conductivity measurements (16 days vs. over 95 days) showed a decrease of up to two orders of magnitude at the longer curing age.

2. For the mix designs investigated, UCS measurements on control specimens showed a decreasing trend, as a result of increase in w/c ratio. The difference between UCS values of immature and mature specimens were negligible. This was potentially because

immature specimens were tested at an age of 60 days, when likely a considerable amount of hydration process was complete. A parallel test was conducted to compare the UCS values at short (16 days) and long (241 days) curing ages. These tests showed an increase of up to 52 percent in the values as a result of the curing process.

3. Both minor reductions and increases of up to 5250 times were observed in the hydraulic conductivity values after f/t exposure. While the increase in the hydraulic conductivity is a result of formation of cracks and micro-cracks in the specimens due to the freezing process, reduction in the hydraulic conductivity values may be a result of the continued hydration of cement that offsets the deteriorating effect of f/t cycles.

4. Mature specimens exhibited higher increases in the hydraulic conductivity values after f/t exposure as compared to immature exposed specimens. This is likely due to brittleness of the specimens at mature conditions that makes them more susceptible to induced deformations during the freezing action. A continuing hydration process can also reduce the observed changes in the hydraulic conductivity of immature specimens after f/t exposure.

5. Brushing tests were performed at the end of each thawing phase, and the mass loss for each specimen was monitored for twelve cycles of f/t. Mass loss ranged from 0.72 to 23.4 percent, with most of the observed values under 7 percent. Mature specimens showed higher amount of surface damage (mass loss) compared to immature specimens exposed to f/t cycles. Comparing mass loss data with hydraulic conductivity changes after f/t cycles showed the changes are not proportional. This suggests mass loss is not a

credible indicator for predicting changes in the hydraulic conductivity of cement-stabilized soils exposed to f/t cycles.

6. Changes in UCS values were monitored for different specimens exposed to f/t cycles. Decreases of up to 58 percent and increases of up to 14 percent were observed compared to control conditions. No obvious pattern in the changes was observed. Also comparing the results to the hydraulic conductivity measurements didn't show any correlation between the values.

7. Results of hydraulic conductivity measurements after a post exposure healing period of over 120 days showed that depending on the amount of initial damage, some reduction in hydraulic conductivity values can be expected over time. Specimens with lower amounts of damage (i.e. lower increase in hydraulic conductivity values) demonstrated a better potential in terms of reduction in the hydraulic conductivity values after the healing period. However, none of the specimens could achieve full recovery of the hydraulic conductivity values as compared to measurements performed for control conditions.

5. ACKNOWLEDGEMENTS

The funding for this project was provided by NSERC through the NSERC CREATE and Discovery grant programs. The authors would like to thank Mitch Woodworth for assistance in the laboratory.

6. REFERENCES

Abrams, D.A., 1919. *Design of concrete mixtures*, Chicago, IL: Bulletin No. 1, Published by Structural Materials Research Laboratory, Lewis Institute.

ACI, 1990. *Report on soil cement*, Farmington Hills, MI: American Concrete Institute (ACI) Committee 230, ACI230.1R-90.

Aderibigbe, D.A., Akeju, T.A.I. and Orangun, C.O., 1985. Optimal water/cement ratios and strength characteristics of some local clay soils stabilized with cement. *Materials and Structures*, **18**(104):pp.103–108. doi:10.1007/bf02473376.

ASTM-D2487, 2011. Standard practice for classification of soils for engineering purposes (unified soil classification system). In *Annual Book of ASTM Standards*. West Conshohocken, PA: ASTM International. doi:10.1520/d2487-11.

ASTM-D5084, 2010. Standard test methods for measurement of hydraulic conductivity of saturated porous materials using a flexible wall permeameter. In *Annual Book of ASTM Standards*. West Conshohocken, PA: ASTM International. doi:10.1520/d5084-10.

ASTM-D558, 2011. Standard test methods for moisture-density (unit weight) relations of soil-cement. In *Annual Book of ASTM Standards*. West Conshohocken, PA: ASTM International. doi:10.1520/d0558-11.

ASTM-D560, 2003. Standard test methods for freezing and thawing compacted soil-cement mixtures. In *Annual Book of ASTM Standards*. West Conshohocken, PA: ASTM International. doi:10.1520/d0560-03.

ASTM-D6913, 2004. Standard test methods for particle-size distribution (gradation) of soils using sieve analysis. In *Annual Book of ASTM Standards*. West Conshohocken, PA: ASTM International. doi:10.1520/d6913-04r09.

Bellezza, I. and Fratalocchi, E., 2006. Effectiveness of cement on hydraulic conductivity of compacted soil–cement mixtures. *Ground Improvement*, **10**(2):pp.77–90. doi:10.1680/grim.2006.10.2.77.

Boynton, S.S. and Daniel, D.E., 1985. Hydraulic conductivity tests on compacted clay. *ASCE Journal of Geotechnical Engineering*, **111**(4):pp.465–478. doi:10.1061/(asce)0733-9410(1985)111:4(465).

Dempsey, B.J. and Thompson, M.R., 1973. Vacuum saturation method for predicting freeze-thaw durability of stabilized materials. In *Highway Research Record 442*. Highway Research Board, US National Research Council, pp. 44–57.

Edvardsen, C., 1999. Water permeability and autogenous healing of cracks in concrete. *ACI Materials Journal*, **96**(4):pp.448–54.

Eigenbrod, K.D., 2003. Self-healing in fractured fine-grained soils. *Canadian Geotechnical Journal*, **40**:pp.435–449. doi:10.1139/t02-110.

El-Korchi, T., Gress, D., Baldwin, K. and Bishop, P., 1989. Evaluating the freeze-thaw durability of Portland cement-stabilized-solidified heavy metal waste using acoustic measurements. In *Environmental Aspects of Stabilization and Solidification of Hazardous and Radioactive Wastes (STP 1033)*. Edited by P. Côté & M. Gilliam. Philadelphia, PA: ASTM International, pp. 184–191. doi:10.1520/stp22878s.

Ganjian, E., Claisse, P.A., Tyrer, M. and Atkinson, A., 2004. Selection of cementitious mixes as a barrier for landfill leachate containment. *ASCE Journal of materials in civil engineering*, **16**(5):pp.477–486. doi:10.1061/(asce)0899-1561(2004)16:5(477).

Guney, Y., Aydilek, A.H. and Demirkan, M.M., 2006. Geoenvironmental behavior of foundry sand amended mixtures for highway subbases. *Waste Management*, **26**(9):pp.932–45. doi:10.1016/j.wasman.2005.06.007.

Hammad, A., 2013. *Evaluation of soil-cement properties with electrical resistivity*. M.A.Sc. Thesis, Civil and Resource Engineering Department, Dalhousie Univesity, Halifax, NS.

Haug, M.D. and Wong, L.C., 1992. Impact of molding water content on hydraulic conductivity of compacted sand-bentonite. *Canadian Geothechnical Journal*, **29**:pp.253–262. doi:10.1139/t92-029.

Hearn, N., Hooton, R.D. and Nokken, M.R., 2006. Pore structure, permeability, and penetration resistance characteristics of concrete. In *Significance of Tests and Properties of Concrete and Concrete-Making Materials (STP 169C)*. Edited by J. F. Lamond & J. H. Pielert. West Conshohocken, PA: ASTM International, pp. 238–252. doi:10.1520/stp36424s.

Horpibulsuk, S., Miura, N. and Nagaraj, T.S., 2003. Assessment of Strength Development in Cement-Admixed High Water Content Clays with Abrams' Law as a Basis (Technical Note). *Géotechnique*, **53**(4):pp.439–444.

Horpibulsuk, S., Rachan, R., Chinkulkijniwat, A., Raksachon, Y. and Suddeepong, A., 2010. Analysis of strength development in cement-stabilized silty clay from microstructural considerations. *Construction and Building Materials*, **24**(10):pp.2011–2021. doi:10.1016/j.conbuildmat.2010.03.011.

ITRC, 2011. *Development of performance specifications for solidification/stabilization (technical/regulatory guidance)*, Washington, DC: The Interstate Technology & Regulatory Council, Solidification/Stabilization Team.

Jacobsen, S., Marchand, J. and Homain, H., 1995. SEM observations of the microstructure of frost deteriorated and self-healed concretes. *Cement and Concrete Research*, **25**(8):pp.1781–1790. doi:10.1016/0008-8846(95)00174-3.

Jacobsen, S. and Sellevold, E.J., 1996. Self healing of high strength concrete after deterioration by freeze/thaw. *Cement and Concrete Research*, **26**(I):pp.55–62.

Jolous Jamshidi, R., 2014. *Evaluation of cement-treated soils subjected to cycles of freezing and thawing*. Ph.D. dissertation, Civil and Resource Engineering Department, Dalhousie University, Halifax, Nova Scotia.

Kosmatka, H., Kerkhoff, B. and Panarese, W.C., 2003. *Design and control of concrete mixtures* 14th editi., Skokie, IL: Portland Cement Assosiation.

Mitchell, J.K., Hooper, D.R. and Campanella, R.G., 1965. Permeability of compacted clay. *Journal of Soil Mechanics & Foundations Division, Proceedings of the ASCE,* **91**(SM4):pp.41–65.

Othman, M.A., Benson, C.H., Chamberlain, E.J. and Zimmie, T.F., 1994. Laboratory testing to evaluate changes in hydraulic conductivity of compacted clays caused by freeze-thaw: state-of-the-art. In *Hydraulic Conductivity and Waste Contaminant Transport in Soil (STP 1142)*. Edited by D. E. Daniel & S. J. Trautwein. Philadelphia, PA: ASTM International, pp. 227–254. doi:10.1520/stp23890s.

Pamukcu, S., Topcu, I.B. and Guven, C., 1994. Hydraulic conductivity of solidified residue mixtures used as a hydraulic barrier. In *Hydraulic Conductivity and Waste Contaminant Transport in Soil (STP 1142)*. Edited by D. E. Daniel & S. J. Trautwein. Philadelphia, PA: ASTM International, pp. 505–520. doi:10.1520/stp23905s.

Paria, S. and Yuet, P., 2006. Solidification/stabilization of organic and inorganic contaminants using Portland cement: a literature review. *Journal of Environmental Reviews*, **14**:pp.217–255. doi:10.1139/a06-004.

Popovics, S. and Ujhelyi, J., 2008. Contribution to the concrete strength versus water-cement ratio relationship. *ASCE Journal of Materials in Civil Engineering*, **20**(7):pp.459–464. doi:10.1061/(asce)0899-1561(2008)20:7(459).

Powers, T.C., Copeland, L.E., Hayes, J.C. and Mann, H.M., 1954. Permeability of portland cement paste. *Journal of American Concrete Institute*, **51**:pp.285–298.

Powers, T.C., Copeland, L.E. and Mann, H.M., 1959. *Capillary continuity or discontinuity in cement paste*, Skokie, IL: Bulletin no. 10, Portland Cement Association Research and Development Laboratories.

Powers, T.C. and Helmuth, R.A., 1953. Theory of volume changes in hardened portland-cement paste during freezing. In *Proceedings of the Thirty-Second Annual Meeting of the Highway Research Board*. Edited by F. Burggra & W. J. Miller. Washington, D.C., pp. 285–297.

Powers, T.C. and Willis, T.F., 1949. The air requirement of frost-resistant concrete. In *Proceedings of the Twenty-Ninth Annual Meeting of the Highway Research Board*. Edited by R. W. Crum, F. Burggraf, & W. N. Carey. Washington, D.C., pp. 184–211.

Shea, M.S., 2011. *Hydraulic conductivity of cement-treated soils and aggregates after freezing*. M.A.Sc. thesis, Department of Civil and Environmental Engineering, Brigham Young University, Provo, UT.

Yang, Y., Lepech, M.D., Yang, E.-H. and Li, V.C., 2009. Autogenous healing of engineered cementitious composites under wet–dry cycles. *Cement and Concrete Research*, **39**(5):pp.382–390. doi:10.1016/j.cemconres.2009.01.013.

Figure captions

Figure 1: Effect of mix design on hydraulic and strength performance of cement-stabilized soils. Note: hatched areas represent water contents that are 2 to 6% above optimum water content.

Figure 2: Summary of the testing procedures for a) immature b) mature tests.

Figure 3: Effect of curing age on the compressive strength of cement-stabilized soils.

Figure 4: Hydraulic conductivity ratio (top) and exposed hydraulic conductivity (bottom) for exposed specimens. Note: Vertical solid line represents the OWC conditions.

Figure 5: Variation of hydraulic conductivity ratios after f/t exposure compared to initial hydraulic conductivity values.

Figure 6: Mass loss of the exposed specimens at the end of the 12^{th} cycle of freezing/thawing.

Figure 7: Unconfined compressive strength ratio (top) and residual compressive strength (bottom) of specimens after f/t exposure. Note: Vertical solid line represents the OWC conditions.

Figure 8: Correlation of UCS values for exposed and unexposed conditions.

Figure 9: Hydraulic conductivity recovery of exposed specimens after post-exposure healing period.

Table 1: Summary of soil particle size distributions and w/c ratios used for different mix designs.

Soil name	Mix designation	Water/cement ratio	Mixing method	Soil composition by dry weight, %					USCS classification of blended soil
				Soil A				Soil B	
				9.5-4.75 mm	4.75-1.20 mm	1.20-0.30 mm	0.30-0.08 mm	<0.08 mm	
Soil I (SI)	SI(1)	1	Compaction	13	42	30	15	0	Well graded sand
	SI(1.5)	1.5	Self-consolidation						
	SI(2)	2	Self-consolidation						
Soil II (SII)	SII(1)	1	Compaction	11	36	25	13	15	Silty sand
	SII(1.5)	1.5	Compaction						
	SII(2)	2	Self-consolidation						
Soil III (SIII)	SIII(1)	1	Compaction	9	30	21	10	30	Silty sand
	SIII(1.5)	1.5	Compaction						
	SIII(2)	2	Self-consolidation						

Table 2: Mineral oxides analysis of the soils used in the study.

Mineral oxide	Soil A Wt. %	Soil B Wt. %
Al_2O_3	14.57	15.31
CaO	0.49	1.85
Fe_2O_3	2.66	5.66
K_2O	3.27	4.02
MgO	0.61	1.60
MnO	0.09	0.12
Na_2O	3.03	3.08
P_2O_5	0.23	0.39
SiO_2	71.82	65.65
LOI (1000°C)*	2.41	1.17
Total	99.18	98.85

*LOI: Loss on ignition

Table 3: Details of testing on specimens from each mix design.

Specimen #	Immature exposure conditions							Mature exposure conditions						
	Hydraulic conductivity, unexposed	F/t exposure	Brushing test	Hydraulic conductivity, exposed	UCS, unexposed	UCS, exposed	Hydraulic conductivity, after healing	Hydraulic conductivity, unexposed	F/t exposure	Brushing test	Hydraulic conductivity, exposed	UCS, unexposed	UCS, exposed	Hydraulic conductivity, after healing
1 & 2	X	X		X			X							
3 & 4		X	X			X								
5 & 6					X									
7 & 8								X	X		X			X
9 & 10									X	X			X	
11 & 12												X		

Table 4: Summary of percent mass loss data due to brushing of specimens at different f/t cycles.

SI												
	w/c=1				w/c=1.5				w/c=2			
	Immature		Mature		Immature		Mature		Immature		Mature	
f/t cycles	Average Δ_m	Standard deviation	Average Δ_m	Standard deviation	Average Δ_m	Standard deviation	Average Δ_m	Standard deviation	Average Δ_m	Standard deviation	Average Δ_m	Standard deviation
0	0.00	0.00	0.00	0.00	0.00	0.00	0.00	0.00	0.00	0.00	0.00	0.00
1	0.72	0.03	0.93	0.08	0.14	0.04	0.44	0.10	0.51	0.16	0.39	0.12
2	0.84	0.05	1.23	0.22	0.34	0.09	0.60	0.09	0.89	0.22	0.70	0.30
3	0.91	0.08	1.46	0.33	0.48	0.10	0.83	0.19	1.25	0.14	0.97	0.50
4	0.95	0.11	1.69	0.38	0.68	0.09	1.45	0.00	1.62	0.20	1.47	0.81
5	0.86	0.17	1.97	0.24	0.87	0.04	1.74	0.00	1.92	0.21	1.81	0.96
6	0.92	0.17	1.98	0.38	0.99	0.08	2.03	0.00	2.07	0.24	2.45	1.38
7	0.90	0.21	2.20	0.44	1.19	0.11	2.39	0.00	2.38	0.24	2.66	1.58
8	0.99	0.20	2.38	0.50	1.33	0.17	2.59	0.00	2.70	0.33	2.91	1.72
9	1.02	0.21	2.43	0.49	1.41	0.12	2.74	0.00	2.82	0.27	3.18	1.97
10	1.05	0.21	2.56	0.52	1.59	0.19	2.98	0.01	3.02	0.27	3.41	2.04
11	1.08	0.28	2.70	0.57	1.71	0.13	3.21	0.01	3.60	0.52	3.78	2.32
12	1.15	0.28	2.88	0.59	1.83	0.14	3.36	0.01	3.87	0.27	4.17	2.66
SII												
	w/c=1				w/c=1.5				w/c=2			
	Immature		Mature		Immature		Mature		Immature		Mature	
f/t cycles	Average Δ_m	Standard deviation	Average Δ_m	Standard deviation	Average Δ_m	Standard deviation	Average Δ_m	Standard deviation	Average Δ_m	Standard deviation	Average Δ_m	Standard deviation
0	0.00	0.00	0.00	0.00	0.00	0.00	0.00	0.00	0.00	0.00	0.00	0.00
1	0.66	0.04	0.76	0.35	0.09	0.01	0.54	0.05	-0.01	0.04	0.05	0.05
2	0.95	0.03	1.11	0.36	0.26	0.01	0.75	0.06	0.13	0.01	0.18	0.05
3	1.04	0.02	1.42	0.43	0.35	0.02	0.94	0.05	0.25	0.03	0.08	0.02
4	1.12	0.05	1.64	0.37	0.49	0.02	1.12	0.03	0.37	0.10	0.05	0.01
5	1.21	0.02	1.74	0.37	0.51	0.01	1.24	0.03	0.44	0.13	0.08	0.08
6	1.30	0.01	1.93	0.39	0.56	0.02	1.23	0.02	0.68	0.15	0.12	0.10
7	1.38	0.07	2.01	0.44	0.57	0.02	1.35	0.03	0.75	0.16	0.50	0.03
8	1.41	0.06	2.19	0.44	0.60	0.02	1.36	0.04	0.87	0.12	2.47	1.88
9	1.51	0.09	2.27	0.48	0.61	0.02	1.41	0.02	0.91	0.14	5.19	4.50
10	1.51	0.05	2.33	0.47	0.64	0.01	1.47	0.01	1.11	0.17	9.05	7.63
11	1.60	0.04	2.50	0.45	0.68	0.04	1.50	0.03	1.80	0.46	22.57	1.12
12	1.66	0.03	2.57	0.50	0.72	0.03	1.52	0.04	1.90	0.46	23.40	1.50
SIII												
	w/c=1				w/c=1.5				w/c=2			
	Immature		Mature		Immature		Mature		Immature		Mature	
f/t cycles	Average Δ_m	Standard deviation	Average Δ_m	Standard deviation	Average Δ_m	Standard deviation	Average Δ_m	Standard deviation	Average Δ_m	Standard deviation	Average Δ_m	Standard deviation
0	0.00	0.00	0.00	0.00	0.00	0.00	0.00	0.00	0.00	0.00	0.00	0.00
1	0.38	0.11	0.61	0.10	0.72	0.01	0.90	0.14	0.56	0.04	0.51	0.01
2	0.47	0.12	1.06	0.27	0.87	0.03	1.08	0.16	0.68	0.04	0.90	0.08
3	0.56	0.15	1.30	0.31	0.98	0.09	1.26	0.18	0.81	0.05	1.21	0.12
4	0.70	0.16	1.44	0.29	1.12	0.08	1.36	0.20	0.97	0.08	1.43	0.22
5	0.80	0.20	1.50	0.24	1.15	0.09	1.46	0.20	1.05	0.07	1.47	0.27
6	0.88	0.25	1.64	0.23	1.20	0.13	1.60	0.21	1.15	0.08	1.59	0.31
7	0.94	0.28	1.68	0.29	1.29	0.14	1.66	0.19	1.29	0.07	1.78	0.36
8	0.93	0.28	1.74	0.73	1.32	0.16	1.80	0.18	1.33	0.08	1.84	0.40
9	0.98	0.20	1.83	0.74	1.40	0.19	1.84	0.13	1.43	0.09	1.89	0.41
10	1.13	0.34	1.85	0.76	1.43	0.20	1.85	0.15	1.41	0.11	1.99	0.47
11	1.12	0.37	2.00	0.78	1.43	0.20	2.04	0.11	1.47	0.12	2.18	0.53
12	1.23	0.45	2.01	0.77	1.47	0.21	2.07	0.13	1.54	0.11	2.29	0.58

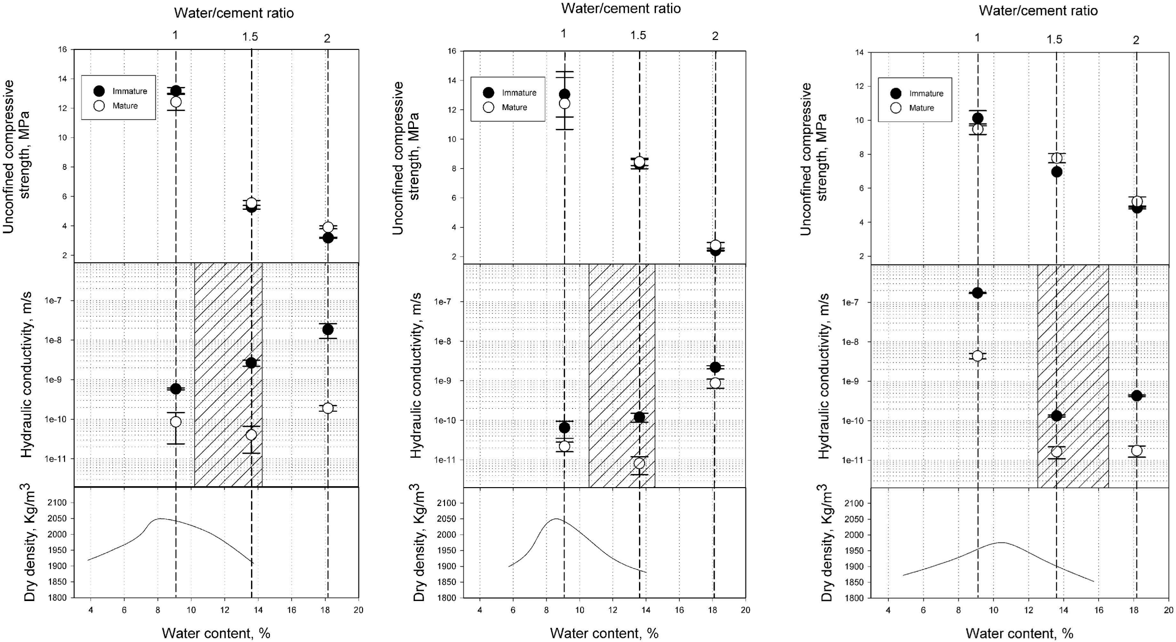

(a) Soil I: 0% fines

(b) Soil II: 15% fines

(c) Soil III: 30% fines

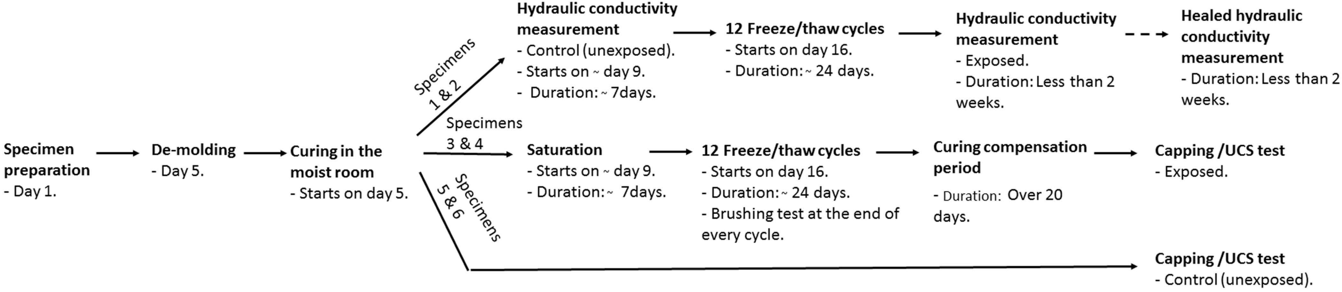
Specimen preparation
- Day 1.
De-molding
- Day 5.
Curing in the moist room
- Starts on day 5.
Specimens 1 & 2
Hydraulic conductivity measurement
- Control (unexposed).
- Starts on ~ day 9.
- Duration: ~ 7days.
12 Freeze/thaw cycles
- Starts on day 16.
- Duration: ~ 24 days.
Hydraulic conductivity measurement
- Exposed.
- Duration: Less than 2 weeks.
Healed hydraulic conductivity measurement
- Duration: Less than 2 weeks.
Specimens 3 & 4
Saturation
- Starts on ~ day 9.
- Duration: ~ 7days.
12 Freeze/thaw cycles
- Starts on day 16.
- Duration: ~ 24 days.
- Brushing test at the end of every cycle.
Curing compensation period
- Duration: Over 20 days.
Capping /UCS test
- Exposed.
Specimens 5 & 6
Capping /UCS test
- Control (unexposed).

(a)

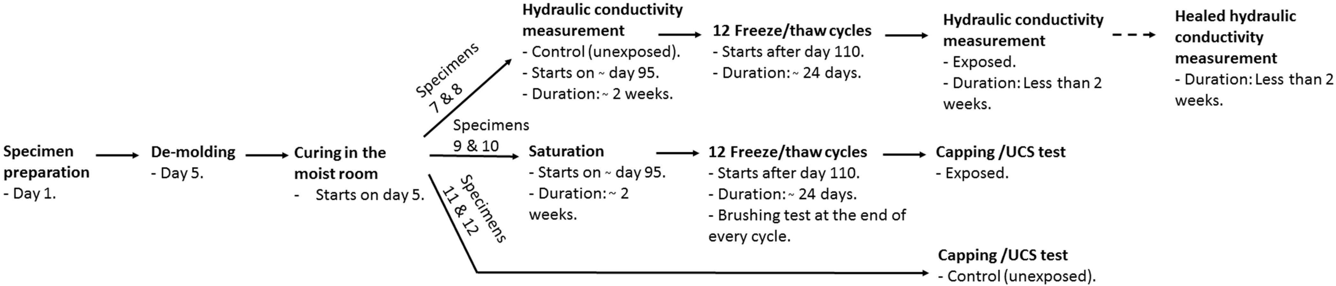
Specimen preparation
- Day 1.
De-molding
- Day 5.
Curing in the moist room
- Starts on day 5.
Specimens 7 & 8
Hydraulic conductivity measurement
- Control (unexposed).
- Starts on ~ day 95.
- Duration: ~ 2 weeks.
12 Freeze/thaw cycles
- Starts after day 110.
- Duration: ~ 24 days.
Hydraulic conductivity measurement
- Exposed.
- Duration: Less than 2 weeks.
Healed hydraulic conductivity measurement
- Duration: Less than 2 weeks.
Specimens 9 & 10
Saturation
- Starts on ~ day 95.
- Duration: ~ 2 weeks.
12 Freeze/thaw cycles
- Starts after day 110.
- Duration: ~ 24 days.
- Brushing test at the end of every cycle.
Capping /UCS test
- Exposed.
Specimens 11 & 12
Capping /UCS test
- Control (unexposed).

(b)

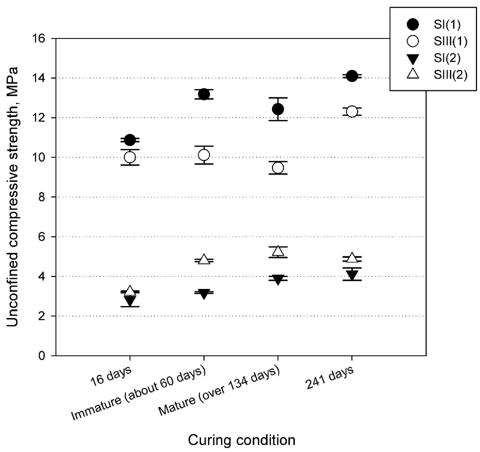
SI(1)
SIII(1)
SI(2)
SIII(2)
Unconfined compressive strength, MPa
0
2
4
6
8
10
12
14
16
16 days
Immature (about 60 days)
Mature (over 134 days)
241 days
Curing condition

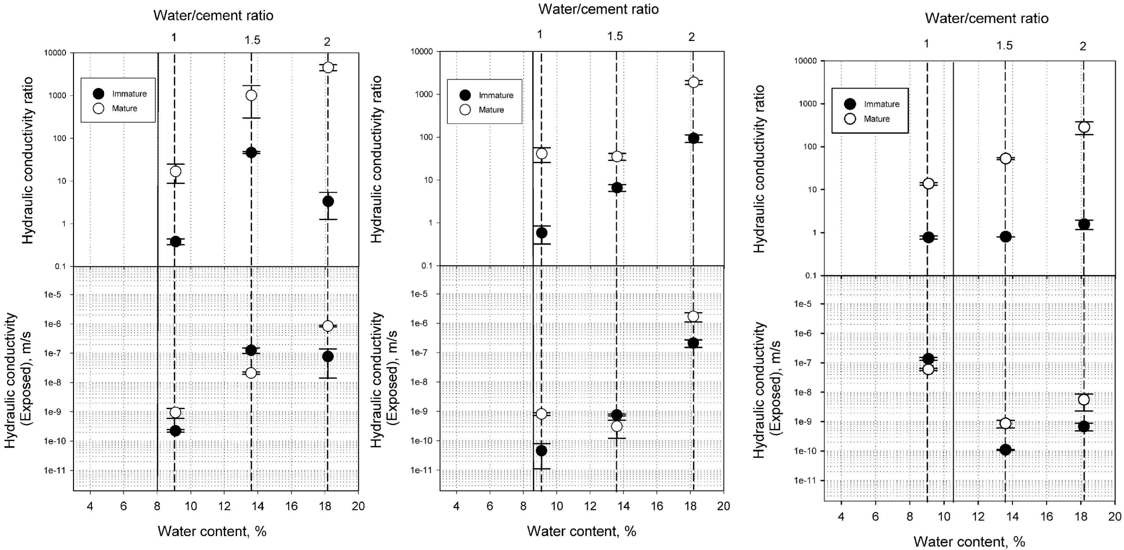

(a) Soil I: 0% fines

(b) Soil II: 15% fines

(c) Soil III: 30% fines

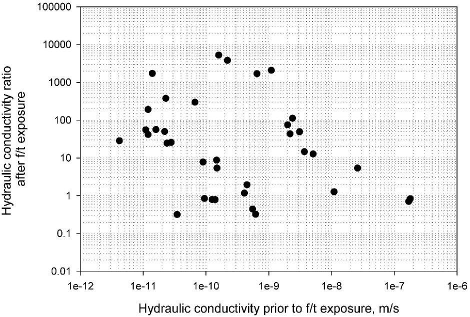
100000
10000
1000
100
10
1
0.1
0.01
Hydraulic conductivity ratio after f/t exposure
1e-12
1e-11
1e-10
1e-9
1e-8
1e-7
1e-6
Hydraulic conductivity prior to f/t exposure, m/s

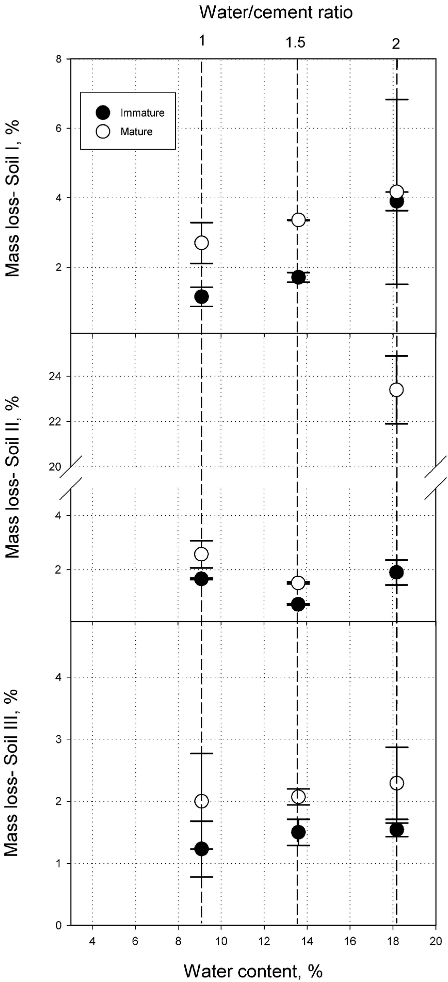

Water/cement ratio
1
1.5
2
Immature
Mature
Mass loss- Soil I, %
Mass loss- Soil II, %
Mass loss- Soil III, %
Water content, %

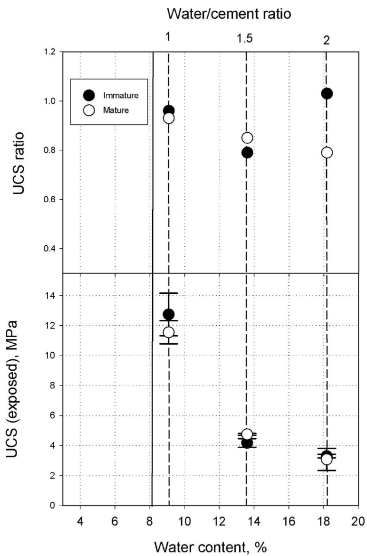

(a)

Soil I: 0% fines

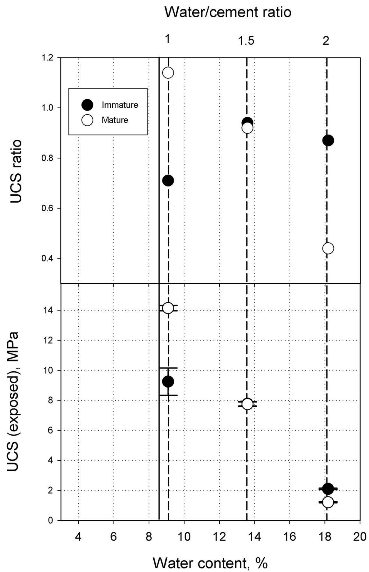

(b)

Soil II: 15% fines

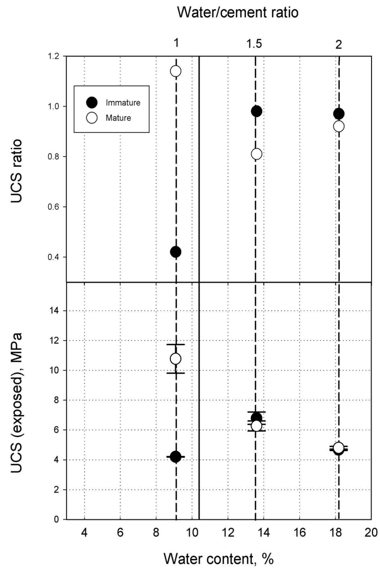

(c)

Soil III: 30% fines

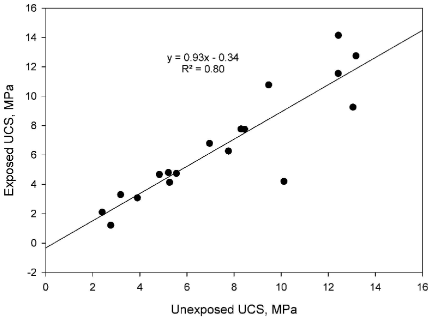

y = 0.93x - 0.34
R² = 0.80
Exposed UCS, MPa
Unexposed UCS, MPa
16
14
12
10
8
6
4
2
0
-2
0
2
4
6
8
10
12
14
16

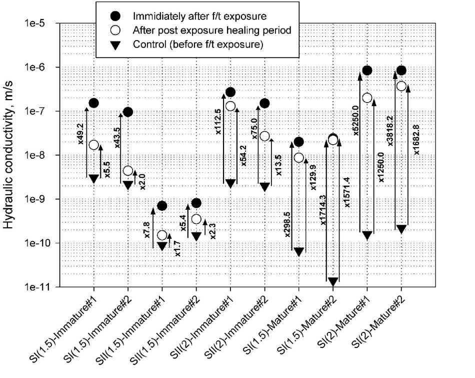

Immidiately after f/t exposure
After post exposure healing period
Control (before f/t exposure)
Hydraulic conductivity, m/s
1e-5
1e-6
1e-7
1e-8
1e-9
1e-10
1e-11
x49.2
x5.5
x43.5
x2.0
x7.8
x1.7
x5.4
x2.3
x112.5
x54.2
x75.0
x13.5
x298.5
x129.9
x1714.3
x1571.4
x5250.0
x1250.0
x3818.2
x1682.8
SI(1.5)-Immature#1
SI(1.5)-Immature#2
SII(1.5)-Immature#1
SII(1.5)-Immature#2
SII(2)-Immature#1
SII(2)-Immature#2
SI(1.5)-Mature#1
SI(1.5)-Mature#2
SI(2)-Mature#1
SI(2)-Mature#2